


 Cite this: *RSC Adv.*, 2025, **15**, 48188

## Hydrothermal synthesis of conductive copper nanowires: effect of oleylamine and dextrose concentrations

Gopu J, † Shriya Musunuri and Krishna C. Etika \*

One-dimensional (1-D) metallic nanoparticles (*i.e.*, nanowires, nanorods) exhibit unique properties and are useful in a variety of applications. 1-D copper nanowires (CuNWs) exhibit excellent electrical conductivity making them an economical alternative in applications that typically employ silver or gold nanowires. In this study, CuNWs were synthesized *via* an environmentally benign and scalable hydrothermal synthesis method using CuCl<sub>2</sub> (CuP) as a copper precursor. Oleylamine (OAm) and dextrose (D) were employed as capping and reducing agents, respectively. The focus of this work was to investigate the influence of varying CuP:OAm and CuP:D molar ratios during synthesis on the nanowire growth, morphology, and electrical conductivity. A series of synthesis trials were conducted by only varying CuP:OAm or CuP:D molar ratios, while keeping all other reaction conditions constant. Morphological analysis of the synthesized products suggests that both OAm and D are essential for the formation of CuNWs. A synthesis conducted at a 1:3.75:1.1 CuP:OAm:D molar ratio produced nanowires with average diameter of 96 nm, while higher OAm concentration resulted in CuNWs with larger diameters. X-ray diffraction analysis confirmed the crystalline nature of the synthesized CuNWs, with diffraction peaks corresponding well to those of FCC copper. The capping of CuNWs with OAm was confirmed through FTIR spectroscopy. Thermogravimetric (TGA) studies on CuNWs show that OAm content in CuNWs increases with increasing CuP:OAm molar ratio during synthesis. The electrical conductivity of CuNW pellets was found to decrease with increasing CuP:OAm molar ratio during synthesis. The highest conductivity of  $1.38 \times 10^5$  S cm<sup>-1</sup> was exhibited in the sample made using 1:3.75:1.1 CuP:OAm:D molar ratio. Furthermore, holding CuNWs pellets under ambient conditions for 60 days did not affect their electrical conductivity.

 Received 30th September 2025  
 Accepted 26th November 2025

DOI: 10.1039/d5ra07427d

[rsc.li/rsc-advances](http://rsc.li/rsc-advances)

### Introduction

One dimensional (1D) conductive metal nanoparticles have gained significant attention due to a wide variety of applications in flexible conductors, sensors, solar cells, wearable electronics and transparent conductive materials.<sup>1–5</sup> Their high aspect ratio, large surface-to-volume ratio, and excellent charge transport capabilities make them highly attractive for next-generation electronics and optoelectronic devices.<sup>6,7</sup> A variety of 1-D electrically conductive nanowires of silver<sup>8</sup> (AgNWs), gold<sup>9</sup> (AuNWs) and Indium tin oxide<sup>10</sup> (ITO) have been widely explored for their exceptional electrical conductivity in these applications, however, their scarcity and high cost pose a challenge for large-scale applications.<sup>11</sup> Alternatively, a variety of 1-D carbon nanoparticles, *i.e.*, carbon nanotubes<sup>12</sup> (CNTs), carbon nanofibers<sup>13</sup> (CNFs) *etc.*, have also been explored, but their complex synthesis protocols makes their large scale production

challenging. Therefore, there is a strong motivation to explore other type of 1-D material.

The 1-D copper nanowires<sup>14–16</sup> (CuNWs) exhibit a unique combination of high electrical conductivity, low cost, and abundant availability. Their electrical conductivity is comparable to that of silver nanowires (AgNWs) but offer a considerable cost advantage, making them well-suited for a variety of electronic applications.<sup>17</sup> However, CuNWs exhibit a high susceptibility to oxidation, particularly when compared to their more noble counterparts, such as gold (Au) or silver (Ag) nanowires which severely limits their widespread applicability. This drawback can be overcome by passivating the CuNWs surface to enhance their environmental stability.<sup>18</sup> Hence, CuNWs can be considered as an attractive alternative for low-cost and flexible electronic applications.<sup>19,20</sup>

A major challenge in synthesizing copper nanowires (CuNWs) has been developing a method that is both industrially viable and environmentally benign.<sup>3</sup> Several synthesis methods, including biosynthesis,<sup>21</sup> photochemical,<sup>22</sup> and electrochemical<sup>23</sup> have been explored for CuNWs synthesis. Among these, wet chemical<sup>24</sup> techniques have gained prominence due

Department of Chemical Engineering, BITS Pilani, Pilani Campus, Rajasthan, 333031, India. E-mail: etika.krishna@pilani.bits-pilani.ac.in

† Both authors contributed equally to this work.



to their simplicity, precise control over nanowire dimensions, and scalability for large-scale applications. Early wet-chemical approaches often involved non-aqueous synthesis in organic solvents. While effective, these methods require very high temperatures ( $>180\text{ }^{\circ}\text{C}$ ) and generate significant organic solvent waste, making them less popular due to serious environmental concerns.<sup>25</sup>

An attractive alternative method was to use water as an eco-friendly reaction medium instead of organic solvents. However, the reduction of copper ions was quite challenging owing to their lower reduction potential (*i.e.*, 0.34 V) than other noble metals (for example, Ag (0.80 V), Au (1.42 V), Pt (1.5 V)).<sup>26</sup> To address this limitation, a strong reducing agent like hydrazine is employed.<sup>27</sup> The reaction was also maintained under highly alkaline conditions, which are necessary to prevent copper ion precipitation and thus facilitate the reduction.<sup>28</sup> Despite its merits, this method suffers from significant drawbacks. It necessitates the use of hydrazine, a reducing agent known for its high toxicity and volatility, which poses considerable safety hazards. Furthermore, maintaining the required alkalinity consumes substantial quantities of strong base (*e.g.*, NaOH), leading to significant environmental challenges.<sup>29</sup>

Subsequently, a new method was developed to circumvent the environmental and safety drawbacks of the traditional alkaline aqueous reduction of copper. This solution reduction method produces high aspect ratio copper nanowires without the need for additional alkali and uses a much milder reducing agent. A typical reaction consists of water, Cu(II) salts, glucose, and alkylamines, and carried out at a moderate temperature (90–120 °C).<sup>30</sup> Although environment friendly, this method was not favourable for large-scale synthesis of CuNWs. Consequently, a new hydrothermal method was developed that could produce copper nanowires on a large scale using an electric pressure cooker.<sup>31</sup> Furthermore, controlled conditions of hydrothermal method yield uniform, crystalline, and oxidation-resistant copper nanowires, unlike the broader distributions resulting from less controlled solution reduction techniques.<sup>32,33</sup> Owing to these advantages, the hydrothermal method seems to be one of the most popular methods for large scale synthesis of CuNWs.<sup>34</sup>

It is shown that the reagent (*i.e.*, capping and reducing agents) concentrations can significantly influence the structure and properties of CuNWs. For example, a recent study revealed that the relative Cu:alkylamine (capping agent) ratio governs nanowire formation and diameter. A 1 : 4 ratio produced a high

yield, whereas a 1 : 1 ratio yielded no nanowires.<sup>35</sup> Additionally, longer alkyl chain lengths correlated with the synthesis of smaller-diameter nanowires.<sup>36</sup> Although interesting, these conclusions, arrived *via* a solution reduction method, cannot be directly extrapolated to hydrothermal processes, which operate under very different reaction environments and growth conditions. Consequently, investigations into the hydrothermal synthesis of CuNWs have mainly examined the influence of reaction time, temperature, or the type of capping agent.<sup>37,38</sup> However, these studies have not specifically explored how variations in the concentrations of capping or reducing agents affect CuNW growth and electrical properties, which forms the prime motivation of the present work.

This work reports a study on the hydrothermal synthesis of CuNWs from an aqueous CuCl<sub>2</sub> (CuP) precursor using oleyl-amine (OAm) and dextrose (D) as capping and reducing agents, respectively. The synthesis was performed at varying CuP : OAm and CuP : D ratio and the obtained products were characterized for their morphology, crystal structure and electrical conductivity. Furthermore, the capping layer content on CuNWs was estimated using thermogravimetric studies.

## Materials

Copper(II) chloride dihydrate (CuCl<sub>2</sub> · 2H<sub>2</sub>O), MW = 170.48 g mol<sup>-1</sup>, analytical reagent (AR), 98% pure and Hexane (C<sub>6</sub>H<sub>14</sub>), MW = 86.18 g mol<sup>-1</sup> laboratory reagent (LR) were supplied by Molychem (Maharashtra, India); Dextrose (C<sub>6</sub>H<sub>12</sub>O<sub>6</sub>), MW = 180.16 g mol<sup>-1</sup>, extra pure (AR) and Oleyl amine(C<sub>18</sub>H<sub>37</sub>N), MW = 267.46 g mol<sup>-1</sup> (*cis*-9-octadecenylamine, AR 95% pure) were purchased from SRL chemicals (Maharashtra, India). All the chemicals were used as received without further purification.

## Preparation of copper nanowires

CuNWs were synthesized using a hydrothermal synthesis method reported earlier. The schematic shown in Fig. 1 illustrates the synthesis protocol. Concisely, the required quantity of CuP and D were added to a flask containing 1 L of deionized water and stirred for 10 minutes to form a uniform dispersion. Subsequently, OAm was gradually added to the reaction mixture under continuous magnetic stirring. The flask was then sealed, and the solution temperature was raised to 70 °C, where it was maintained for 12 hours with continuous stirring, resulting in an ashy blue-colored solution. The solution was then transferred

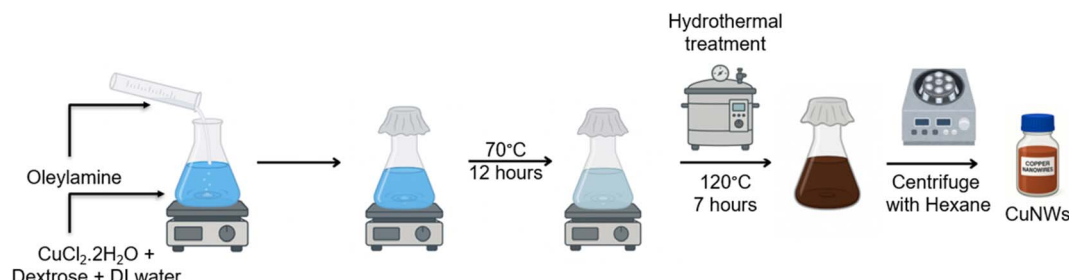


Fig. 1 A schematic illustration of the CuNWs synthesis procedure.



Table 1 Sample codenames, and corresponding reagent concentrations

Sample code	$\text{CuCl}_2 \text{ (mol L}^{-1}\text{)} \times 10^{-3}$	$\text{Oleylamine (mol L}^{-1}\text{)} \times 10^{-3}$	$\text{Dextrose (mol L}^{-1}\text{)} \times 10^{-3}$
OA120D00	20	120	0
OA120D11	20	120	11
OA120D22	20	120	22
OA120D33	20	120	33
OA50D22	20	50	22
OA75D22	20	75	22
OA100D22	20	100	22

into an autoclave reactor (UHPA-22, MAC, India) and heated at 120 °C (198 kPa) for 7 hours before being cooled to room temperature. After autoclaving, a dark brown solution with a reddish-brown sediment at the bottom was obtained. The liquid was carefully removed to isolate the sediment, which was then washed multiple times with hexane and centrifuged at 7500 rpm for 10 minutes to eliminate impurities yielding a reddish-brown powder. The synthesized products were stored under ambient conditions for further testing. Table 1 presents the concentrations of OAm, and dextrose used during synthesis, along with the sample codes of the obtained powders. Anomalously, a white-colored powder was obtained when synthesis was carried out using only OAm and CuP (*i.e.*, in the absence of D).

## Characterization

SEM images were captured using a FE-SEM (Apreo LoVac; FEI; Thermo Fisher) operated at 20 kV accelerating voltage. The images were captured at a constant magnification of 50 000 $\times$  for all the synthesized samples. The XRD analysis was performed using X-ray diffractometer, (D-2 phaser; Bruker). The diffractograms were recorded at a scan rate of 2° min $^{-1}$  over a 2 $\theta$  range of 20° to 80°, using the Cu K $\alpha$  radiation source of wavelength ( $\lambda$ ) = 1.54 Å. For infrared spectroscopy, the CuNW sample was finely ground along with KBr and pressed into a thin pellet. The pellet was then analysed in a FTIR instrument (Frontier; PerkinElmer) and the spectra was recorded in the transmission mode over the wavenumber range of 4000–450 cm $^{-1}$ . The FTIR spectra of pure OAm was obtained through attenuated total reflectance (ATR) method using the same instrument. The thermogravimetric analysis was performed in the temperature range of 30 to 800 °C with a temperature ramp of 10 °C min $^{-1}$  under nitrogen atmosphere using a TGA (4000; PerkinElmer). For the conductivity measurements, the nanowires were densely pressed into a pellet of 13 mm diameter and 80 µm thickness using pellet press. The obtained pellet was used as specimen on the four-point probe (T2001A4; Ossila BV). A total of five locations per pellet were analysed and voltage of 0.1 V was applied for conductivity measurement.

## Results & discussion

The synthesis of metallic nanowires requires two basic components, *i.e.*, a reducing agent and a capping agent.<sup>39</sup> While a reducing agent promotes the conversion of metal ions to their

metallic state, capping agent selectively adsorbs onto specific crystal facets of the growing nuclei, thereby inhibiting further reduction.<sup>40</sup> This promotes the growth along the free facets leading to an anisotropic nanostructure. Therefore, the relative concentrations of reducing or capping agent with respect to the metal precursor are important for growth and morphology control in metallic nanowires.

To investigate the effect of OAm and D on nanowire growth and morphology, CuNWs were synthesized hydrothermally at different CuP : OAm or CuP : D molar ratios, while keeping all other reaction conditions constant. The resulting products were characterized using field-emission scanning electron microscopy (FE-SEM) to examine their microstructural features. The FE-SEM images illustrating the influence of varying the CuP : D molar ratio are presented in Fig. 2, whereas those depicting the effect of different CuP : OAm molar ratios during hydrothermal synthesis are shown in Fig. 3.

In a synthesis conducted with a CuP : OAm molar ratio of 1 : 6 and without D, a white colored powder (*i.e.*, OA120D00) was formed. Fig. 2(a) shows the SEM image of this white powder where the formation of flaky particulates instead of nanowires can be seen. The EDX spectra (shown in Fig. S1) obtained on this powder shows significant amount of chlorine present in the sample, which suggests that these flaky particles may be the crystals of CuCl<sub>2</sub>. Based on these observations, it is reasonable to deduce that the reduction of Cu<sup>2+</sup> to Cu<sup>0</sup> did not occur in the absence of dextrose which acts as a mild reducing agent. In earlier studies employing alkylamines as capping agents, Cu nanowires were reported to form under hydrothermal conditions. Although these studies suggested that alkylamines can themselves act as a mild reducing agents but our results differ from these observations. However, it should be noted that reaction time and temperatures employed in these studies were significantly higher than those used the present work.<sup>41,42</sup> Nevertheless, these results suggest that dextrose may be essential for formation of CuNWs, especially at the conditions employed in this study.

The SEM image of the sample OA120D11, shown in Fig. 2(b), reveals a significant presence of spherical particles compared to those having wire-like morphology. This may result from an insufficient concentration of dextrose, limiting the one-dimensional growth of the particles. In contrast, the SEM image of the sample OA120D22 shown in Fig. 2(c) reveals wire-like particles confirming the successful growth of CuNWs.



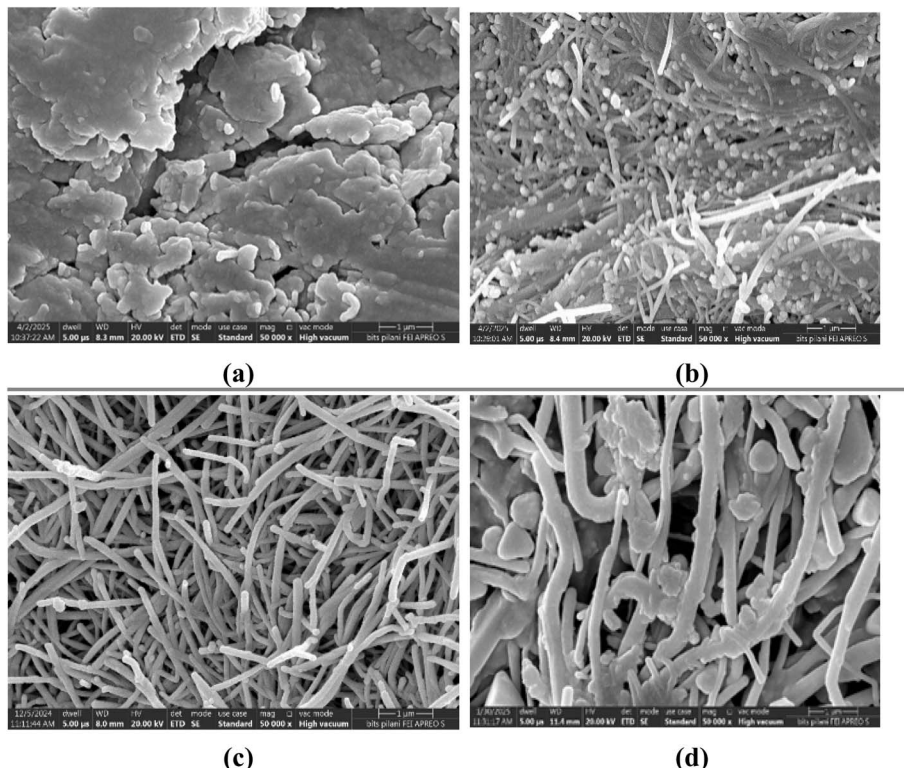


Fig. 2 SEM images of (a) OA120D00, (b) OA120D11, (c) OA120D22, (d) OA120D33.

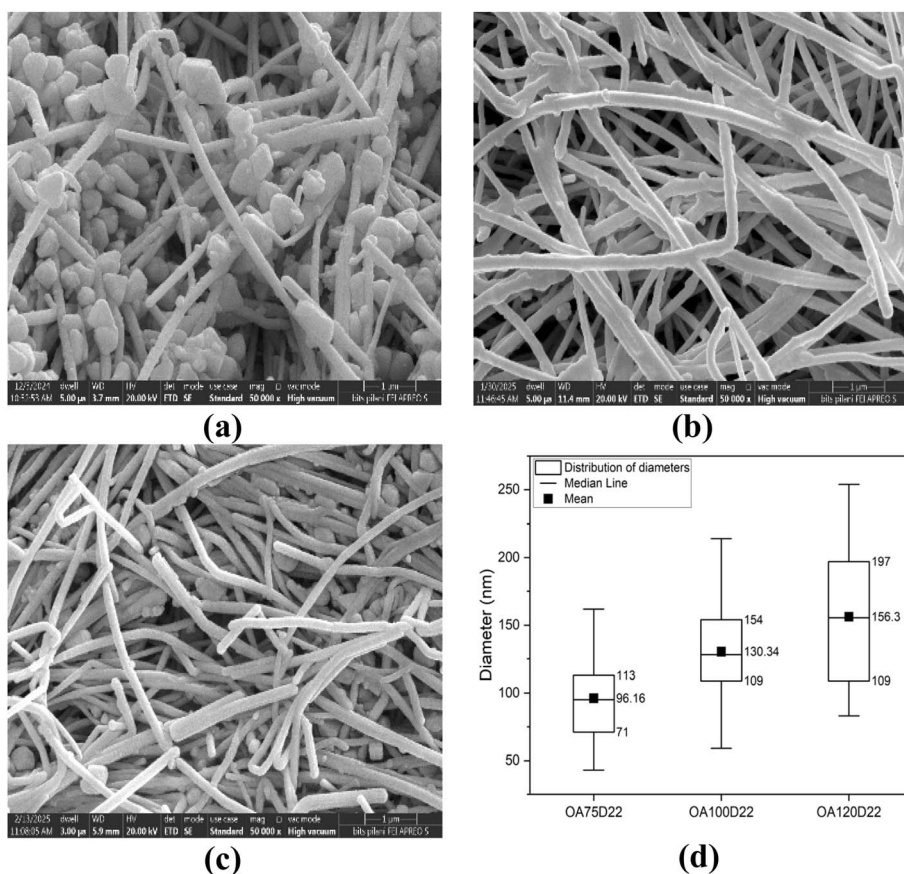


Fig. 3 SEM micrographs of the samples OA50D22 (a), OA75D22 (b), OA100D22 (c) and the corresponding diameter distribution of CuNWs (d).



However, as illustrated in Fig. 2(d) further increasing the dextrose concentration to 33 mmol resulted in excessive clustering and branching of CuNWs, likely attributable to an accelerated reduction rate during the synthesis process. Based on the above results, it can be understood that an optimum concentration of dextrose is required for efficient growth of CuNWs.

To investigate the influence of OAm concentration on CuNW growth, synthesis trials were conducted at different CuP : OAm molar ratios. Since good quality CuNWs were formed at a CuP : D molar ratio of 1 : 1.1, this ratio was maintained in these trials. The SEM images recorded on products obtained from these trials are shown in Fig. 3. The SEM micrograph of the product synthesized at a CuP : OAm molar ratio of 1 : 2.5 (*i.e.*, OA50D22) is shown in Fig. 3(a). The image reveals the formation of a few CuNWs along with a large number of multi-faceted nanoparticles. This may be attributed to insufficient capping of copper nuclei by OAm which limits their anisotropic growth. As seen in Fig. 3(b) and (c), the SEM images of the products synthesized at higher CuP : OAm molar ratios show an increased presence of CuNWs. The average diameter CuNWs were determined through image analysis using Image J software and the results are shown in Fig. 3(d). The average diameters of the CuNWs in samples OA75D22, OA100D22, and OA120D22 were found to be 96 nm, 130 nm, and 156 nm, respectively. These results confirm that CuP : OAm molar ratio in hydrothermal synthesis impacts the resulting CuNWs microstructure. It is interesting to note that increasing CuP : OAm molar ratio during the hydrothermal synthesis resulted in CuNW with larger diameter. However, a contrasting trend was reported for the solution-based reduction method, where higher alkylamine concentrations resulted in thinner nanowires.<sup>33</sup> This difference likely arises from the different nucleation and growth environments in hydrothermal *versus* solution-phase synthesis routes. These observations further our hypothesis that inferences drawn from solution-reduction synthesis cannot be directly extrapolated to hydrothermal system.

To investigate the crystalline structure of the synthesized products, X-ray diffraction (XRD) was performed the results are

shown in Fig. 4. The diffractogram obtained on the samples reveals peaks at  $2\theta$  values of  $43.72^\circ$ ,  $50.82^\circ$ , and  $74.48^\circ$  that are in good agreement with reflections from (111), (200), and (220) planes of FCC copper as per the JCPDS #040836, thereby confirming the presence of Cu in the sample.<sup>43</sup> It can also be seen from Fig. 4 that the most prominent peak corresponded to the (111) plane indicating a directional growth which is known to facilitate the formation elongated nanostructures. One reason for such a directional growth may be the preferential adsorption of OAm on facets with high surface energy compared to (111) plane having lowest surface energy in a FCC structure.<sup>44</sup> The adsorption of OAm inhibits growth along the adsorbed plane thereby promoting the growth along the free surfaces resulting in an anisotropic structure. Furthermore, no additional peaks were observed in the XRD data indicating the absence of any impurities or oxides in the sample confirming the presence of pure and single-phase Cu in the synthesized nanowires.

XRD analysis suggested preferential growth of CuNW along the (111) plane which was attributed to a preferential adsorption of OAm on other facets. To confirm the presence of OAm on the surface of CuNWs, Fourier transform infrared (FTIR) spectroscopy was performed on the synthesized CuNWs and the results are presented in Fig. 5. The transmittance spectra obtained on pure OAm and OA75D22 samples exhibited similar characteristics of N-H and C-H asymmetric stretching vibrations at  $3439\text{ cm}^{-1}$  and  $2920\text{ cm}^{-1}$  respectively, suggesting the presence of amine and alkyl groups.<sup>45</sup> Moreover, the N-H, C-N and C=C bending peaks were also present in both the samples, as shown in Fig. 6.<sup>46</sup> Based on the results obtained, it is reasonable to deduce that the OAm presence on the surface of CuNWs.

The broadening of the N-H stretch peak in the OA75D22 sample, compared to pure OAm, indicates interactions between Cu atoms and the nitrogen in the amine group of OAm, as well as possible hydrogen bonding with nearby amine molecules. This interaction likely contributes to the shift in characteristic peaks, which, as observed in previous studies, can be attributed

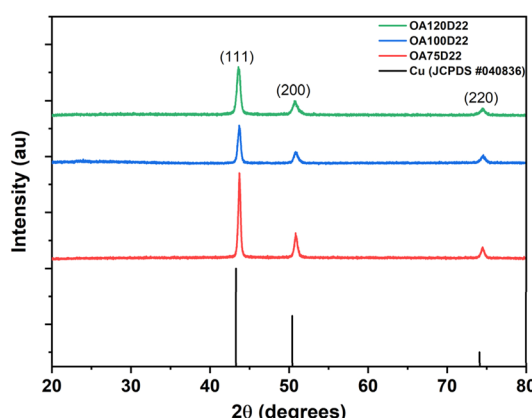


Fig. 4 XRD patterns of synthesized CuNWs along with JCPDS reference for pure Cu.

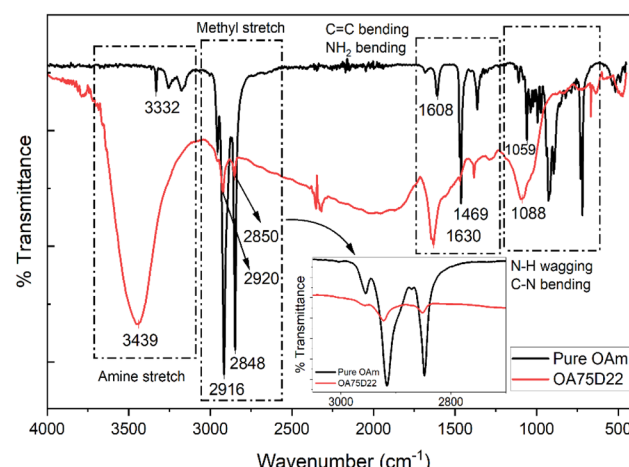


Fig. 5 FTIR spectra of pure OAm and CuNWs synthesized with OAm (OA75D22).



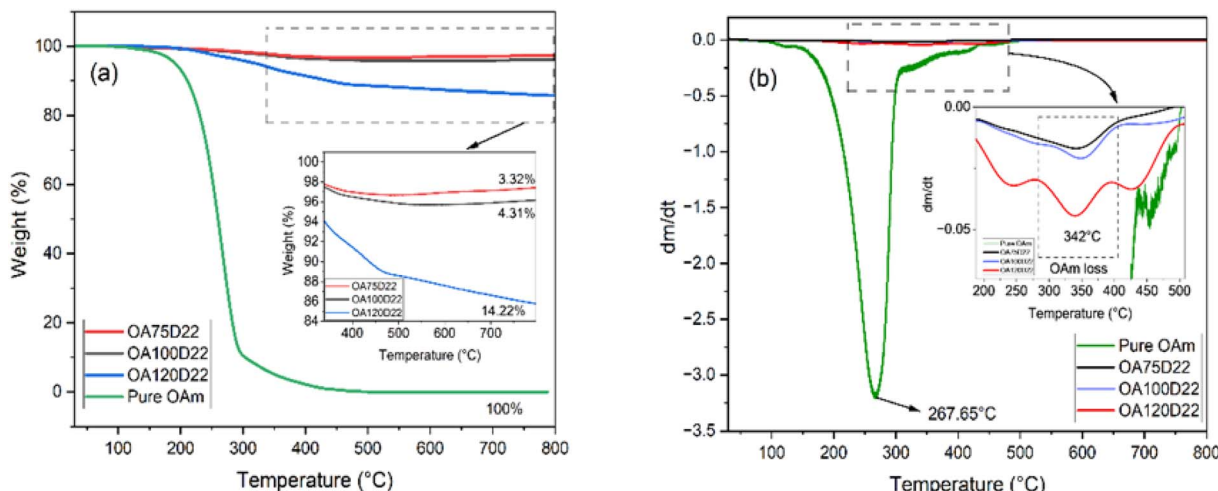


Fig. 6 The percentage weight loss as a function of temperature (a) and the corresponding differential thermogravimetric (DTG) plots of CuNWs and pure OAm (b).

to modifications induced by attachment to the Cu atom surface.<sup>47</sup>

Furthermore, the absence of Cu–O stretching peaks in the 450–630 cm<sup>−1</sup> region in sample suggests that synthesized CuNWs were free of any oxidation. It should be worth noting that both FTIR and XRD analysis confirmed the absence of any oxides in the synthesized sample. These observations, therefore, demonstrate that capping of CuNWs using OAm offers effective passivation that could prevent the oxidation.

The amount of oleylamine (OAm) associated with the CuNWs can be correlated with the thickness of the capping layer. To determine the OAm content on the nanowire surface, thermogravimetric analysis (TGA) under inert (*i.e.*, N<sub>2</sub>) atmosphere was performed and the results are presented in Fig. 6. Copper exhibits good thermal stability under inert conditions, therefore, any weight loss observed in the samples would correspond to the loss of OAm only.<sup>48</sup> It can be seen from Fig. 6 that pure OAm is stable up to 200 °C and exhibits significant degradation around 250 °C and completely degrades at temperature above 400 °C. However, CuNW samples exhibited a gradual and continuous weight loss below 400 °C, indicating the progressive removal of surface-adsorbed species and decomposition of the organic capping layer. The thermogravimetric data reveals distinct differences among the samples, with OA75D22, OA100D22, and OA120D22 showing total weight losses of 3.32%, 4.31%, and 14.22%, respectively. The relatively higher weight loss observed for OA120D22 suggests a greater amount of surface-bound oleylamine, consistent with its higher precursor concentration during synthesis. The observed trend implies that increasing OAm concentration enhances surface coverage and passivation of the CuNWs, which may influence both their thermal stability and oxidation resistance under elevated temperatures.

The observed TGA weight loss can arise from both free (unassociated) and surface-bound (associated) oleylamine (OAm) present in the CuNW samples. To distinguish between these contributions, differential thermogravimetric (DTG)

analysis was performed and the results are shown in Fig. 6(b). The DTG curve shows that pure OAm exhibits a maximum degradation temperature of 267 °C, whereas the CuNW samples exhibits a significantly higher value of ~342 °C. The higher degradation temperature of OAm in the CuNW samples may be attributed to its enhanced resistance to thermal decomposition, likely arising from strong interfacial interactions between OAm molecules and the CuNW surface. Similar behavior has been reported in other metal–amine systems, where coordination or adsorption of amine ligands contributes to improved thermal stability.<sup>49</sup> Based on these results, it can be inferred that increasing the OAm concentration during synthesis leads to the formation of a thicker passivation layer on the CuNW surface.

The presence of a surface passivation layer on the CuNW surface can substantially enhance the junction resistance and thereby reduce the nanowire bulk electrical conductivity, which could potentially limit their applicability.<sup>50</sup> To determine the impact of OAm adherence on CuNWs electrical conductivity, the nanowire powders were pressed to form cylindrical pellets. The DC conductivity was measured on these pellets, and the results are shown in Fig. 7. It should be noted that the conductivities in pellets were relatively lower than that reported for bulk copper. This may be attributed to the presence of an insulating capping layer around CuNWs which increases the resistance for electron transport.<sup>51</sup> Additionally, due to the random alignment of nanowires in the pellets, the flow of electrons is confined at the nanowire junctions leading to increased resistance. Moreover, CuNWs networks may contain voids and discontinuous pathways, where tunnelling gaps between copper segments result in granular metal behaviour rather than the continuous metallic conduction observed in bulk copper.<sup>52</sup> The electrical conductivity of the OA75D22 pellet was measured to be  $1.38 \times 10^5$  S cm<sup>−1</sup>, whereas the pellets derived from OA100D22 and OA120D22 exhibited conductivities lower by approximately one and two orders of magnitude, respectively. These results suggest that an increase in the CuP : OAm ratio during hydrothermal synthesis leads to CuNWs with



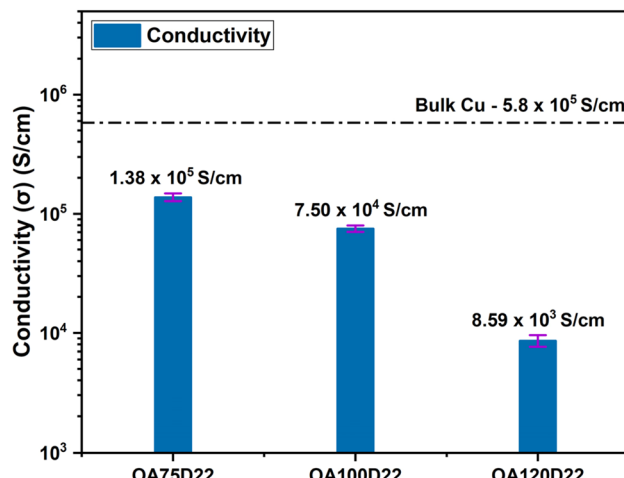


Fig. 7 Electrical conductivity of pellets made using different CuNW samples. The average value obtained for each pellet is displayed at top of each bar.

reduced electrical conductivity, likely due to the formation of a thicker organic capping layer that impedes charge transport. Similar observations were made on silver nanowires (AgNWs).<sup>53</sup> The electrical conductivity of CuNWs stored under ambient conditions typically decreases over time due to surface oxidation, which is a major limitation of copper-based nanowires.<sup>54</sup> However, in the present study, no noticeable reduction in conductivity was observed for the pellets even after 30 and 60 days of storage in air, indicating excellent oxidation resistance. These results further confirm the effectiveness of the OAm capping layer in promoting oxidation resistance in CuNWs.

## Conclusion

In this work, copper nanowires (CuNWs) were synthesized *via* a hydrothermal route using copper(II) chloride (CuP) as the precursor, with oleylamine (OAm) and dextrose (D) serving as the capping and reducing agents, respectively. A series of synthesis trials were performed to investigate the influence of varying CuP:OAm and CuP:D molar ratios on nanowire growth, morphology, and electrical conductivity. The results revealed that both OAm and D are essential for CuNW formation. Synthesis conducted at a CuP:OAm:D molar ratio of 1 : 3.75 : 1.1 yielded nanowires with an average diameter of 96 nm, while higher OAm concentrations produced nanowires of larger diameters. X-ray diffraction confirmed the crystalline nature of the CuNWs, exhibiting diffraction peaks matching with those of FCC copper. FTIR analysis verified the presence of OAm on the nanowire surface, while thermogravimetric analysis (TGA) indicated that the OAm content increased with higher CuP:OAm ratios during synthesis. Electrical conductivity measurements showed a decline in conductivity with increasing OAm concentration, with the highest value of  $1.38 \times 10^5 \text{ S cm}^{-1}$  obtained for the sample synthesized at a 1 : 3.75 : 1.1 CuP:OAm:D ratio. Furthermore, CuNW pellets retained their electrical conductivity even after storage under ambient conditions for 60 days, demonstrating excellent environmental stability.

## Conflicts of interest

There are no conflicts of interest to declare.

## Data availability

The datasets supporting the findings of this study, including raw and processed data from SEM, XRD, FTIR, TGA, and electrical conductivity measurements, are available from the corresponding author upon reasonable request.

The data supporting this article have been included as supplementary information (SI). Supplementary information is available. See DOI: <https://doi.org/10.1039/d5ra07427d>.

## References

- 1 Z. Tang and N. A. Kotov, One-Dimensional Assemblies of Nanoparticles: Preparation, Properties, and Promise, *Adv. Mater.*, 2005, **17**(8), 951–962, DOI: [10.1002/adma.200401593](https://doi.org/10.1002/adma.200401593).
- 2 M. Althumayri, R. Das, R. Banavath, L. Beker and A. M. Achim, Recent Advances in Transparent Electrodes and Their Multimodal Sensing Applications, *Adv. Sci.*, 2024, **11**(38), 2405099, DOI: [10.1002/advs.202405099](https://doi.org/10.1002/advs.202405099).
- 3 X. Li, Y. Wang, C. Yin and Z. Yin, Copper Nanowires in Recent Electronic Applications: Progress and Perspectives, *J. Mater. Chem. C*, 2020, **8**(3), 849–872, DOI: [10.1039/c9tc04744a](https://doi.org/10.1039/c9tc04744a).
- 4 W. Huang, J. Li, S. Zhao, F. Han and G. Zhang, Highly Electrically Conductive and Stretchable Copper Nanowires-Based Composite for Flexible and Printable Electronics, *Compos. Sci. Technol.*, 2017, **146**, 169–176, DOI: [10.1016/j.compscitech.2017.04.030](https://doi.org/10.1016/j.compscitech.2017.04.030).
- 5 O. Ohienko and Y. Oh, Preparation of Narrow Copper Nanowires with Less Oxidized Surface for Flexible and Transparent Electrodes under Octadecylamine, *Mater. Chem. Phys.*, 2020, **246**, 122783, DOI: [10.1016/j.matchemphys.2020.122783](https://doi.org/10.1016/j.matchemphys.2020.122783).
- 6 V. B. Nam and D. Lee, Copper Nanowires and Their Applications for Flexible Transparent Conducting Films : A Review, *Nanomaterials*, 2016, **6**(3), 47, DOI: [10.3390/nano6030047](https://doi.org/10.3390/nano6030047).
- 7 Y. Zhang, J. Guo, D. Xu, Y. Sun and F. Yan, Synthesis of Ultralong Copper Nanowires for High-Performance Flexible Transparent Conductive Electrodes: The Effects of Polyhydric Alcohols, *Langmuir*, 2018, **34**(13), 3884–3893, DOI: [10.1021/acs.langmuir.8b00344](https://doi.org/10.1021/acs.langmuir.8b00344).
- 8 R. Karimi-Chaleshtori, A. H. Nassajpour-Esfahani, M. R. Saeri, P. Rezai and A. Doostmohammadi, Silver Nanowire-Embedded PDMS with High Electrical Conductivity: Nanowires Synthesis, Composite Processing and Electrical Analysis, *Mater. Today Chem.*, 2021, **21**, 100496, DOI: [10.1016/j.mtchem.2021.100496](https://doi.org/10.1016/j.mtchem.2021.100496).
- 9 J. Siegel, J. Heitz, A. Řežníčková and V. Švorčík, Preparation and Characterization of Fully Separated Gold Nanowire Arrays, *Appl. Surf. Sci.*, 2013, **264**, 443–447, DOI: [10.1016/j.apsusc.2012.10.041](https://doi.org/10.1016/j.apsusc.2012.10.041).



10 D. T. Dam, X. Wang and J. M. Lee, Fabrication of a Mesoporous  $\text{Co(OH)}_2$ /ITO Nanowire Composite Electrode and Its Application in Supercapacitors, *RSC Adv.*, 2012, 2(28), 10512–10518, DOI: [10.1039/c2ra21747c](https://doi.org/10.1039/c2ra21747c).

11 Y. Cheng, S. Wang, R. Wang, J. Sun and L. Gao, Copper Nanowire Based Transparent Conductive Films with High Stability and Superior Stretchability, *J. Mater. Chem. C*, 2014, 2(27), 5309–5316, DOI: [10.1039/c4tc00375f](https://doi.org/10.1039/c4tc00375f).

12 G. Sun, G. Chen, Z. Liu and M. Chen, Preparation, Crystallization, Electrical Conductivity and Thermal Stability of Syndiotactic Polystyrene/Carbon Nanotube Composites, *Carbon*, 2010, 48(5), 1434–1440, DOI: [10.1016/j.carbon.2009.12.037](https://doi.org/10.1016/j.carbon.2009.12.037).

13 D. Sebastián, I. Suelves, R. Moliner and M. J. Lázaro, The Effect of the Functionalization of Carbon Nanofibers on Their Electronic Conductivity, *Carbon*, 2010, 48(15), 4421–4431, DOI: [10.1016/j.carbon.2010.07.059](https://doi.org/10.1016/j.carbon.2010.07.059).

14 Y. Xu, S. Li, L. Yin, X. Wu and H. Zhang, Progress on Copper-Based Anode Materials for Sodium-Ion Batteries, *ChemPhysChem*, 2024, 25(17), e202400416, DOI: [10.1002/cphc.202400416](https://doi.org/10.1002/cphc.202400416).

15 P. V. Arsenov, K. S. Pilyushenko, P. S. Mikhailova, M. A. Atlanov, M. A. Popov, N. P. Simonenko, T. L. Simonenko, I. S. Vlasov and I. A. Volkov, Synthesis of Copper Nanowires and Facile Fabrication of Nanostructured Conductors with High Transparency in 400–2500 nm Spectral Range, *Nano-Struct. Nano-Objects*, 2025, 41, 101429, DOI: [10.1016/j.nanoso.2024.101429](https://doi.org/10.1016/j.nanoso.2024.101429).

16 B. Rajesh Kumar and K. C. Etika, Facile One-Pot Hydrothermal Synthesis of Copper Nanowires and Their Impact on the EMI Shielding Capability of Epoxy Composites, *Chem. Eng. Technol.*, 2022, 45(3), 410–416, DOI: [10.1002/ceat.202100389](https://doi.org/10.1002/ceat.202100389).

17 A. R. Rathmell, S. M. Bergin, Y. L. Hua, Z. Y. Li and B. J. Wiley, The Growth Mechanism of Copper Nanowires and Their Properties in Flexible, Transparent Conducting Films, *Adv. Mater.*, 2010, 22(32), 3558–3563, DOI: [10.1002/adma.201000775](https://doi.org/10.1002/adma.201000775).

18 Y. K. Kim, Y. J. Yu, S. H. Kim and J. Y. Choi, Synthesis of High Aspect Ratio Copper Nanowire Using Copper Oxalate Precursor, *J. Mater. Sci.*, 2024, 59(26), 11718–11731, DOI: [10.1007/s10853-024-09834-8](https://doi.org/10.1007/s10853-024-09834-8).

19 S. Yu, J. Li, L. Zhao, M. Wu, H. Dong and L. Li, Simultaneously Enhanced Performances of Flexible CuNW Networks by Covering ATO Layer for Polymer Solar Cells, *Sol. Energy Mater. Sol. Cells*, 2021, 221, 110885, DOI: [10.1016/j.solmat.2020.110885](https://doi.org/10.1016/j.solmat.2020.110885).

20 S. Zhao, F. Han, J. Li, X. Meng, W. Huang, D. Cao, G. Zhang, R. Sun and C. P. Wong, Advancements in Copper Nanowires: Synthesis, Purification, Assemblies, Surface Modification, and Applications, *Small*, 2018, 14(26), 1–30, DOI: [10.1002/smll.201800047](https://doi.org/10.1002/smll.201800047).

21 M. Silva, A. V. Gir, P. A. A. P. Marques and C. S. R. Freire, Bio-Based Synthesis of Oxidation Resistant Copper Nanowires Using an Aqueous, *Plant Extract*, 2019, 221, 122–131, DOI: [10.1016/j.jclepro.2019.02.189](https://doi.org/10.1016/j.jclepro.2019.02.189).

22 Y. Shimotsuma, T. Yuasa, H. Homma, M. Sakakura, A. Nakao, K. Miura and P. G. Kazansky, Photoconversion of copper flakes to nanowires with ultrashort pulse laser irradiation, *Chem. Mater.*, 2007, 19(6), 1206–1208.

23 T. Gao, G. Meng, Y. Wang, S. Sun and L. Zhang, Electrochemical Synthesis of Copper Nanowires, *J. Phys.: Condens. Matter.*, 2002, 14(3), 355.

24 S. Xu, X. Sun, H. Ye, T. You, X. Song and S. Sun, Selective Synthesis of Copper Nanoplates and Nanowires via a Surfactant-Assisted Hydrothermal Process, *Mater. Chem. Phys.*, 2010, 120(1), 1–5, DOI: [10.1016/j.matchemphys.2009.10.049](https://doi.org/10.1016/j.matchemphys.2009.10.049).

25 D. V. Ravi Kumar, K. Woo and J. Moon, Promising Wet Chemical Strategies to Synthesize Cu Nanowires for Emerging Electronic Applications, *Nanoscale*, 2015, 7(41), 17195–17210, DOI: [10.1039/c5nr05138j](https://doi.org/10.1039/c5nr05138j).

26 K. Liu, Z. Qiao and C. Gao, Preventing the Galvanic Replacement Reaction toward Unconventional Bimetallic Core–Shell Nanostructures, *Molecules*, 2023, 28(15), DOI: [10.3390/molecules28155720](https://doi.org/10.3390/molecules28155720).

27 H. Harsojo, L. A. Puspita, D. Mardiansyah, R. Roto and K. Triyana, The Roles of Hydrazine and Ethylenediamine in Wet Synthesis of Cu Nanowire, *Indones. J. Chem.*, 2017, 17(1), 43–48, DOI: [10.22146/ijc.23618](https://doi.org/10.22146/ijc.23618).

28 S. Ye, I. E. Stewart, Z. Chen, B. Li, A. R. Rathmell and B. J. Wiley, How Copper Nanowires Grow and How to Control Their Properties, *Acc. Chem. Res.*, 2016, 49(3), 442–451, DOI: [10.1021/acs.accounts.5b00506](https://doi.org/10.1021/acs.accounts.5b00506).

29 M. Kevin, G. Y. R. Lim and G. W. Ho, Facile Control of Copper Nanowire Dimensions via the Maillard Reaction: Using Food Chemistry for Fabricating Large-Scale Transparent Flexible Conductors, *Green Chem.*, 2015, 17(2), 1120–1126, DOI: [10.1039/c4gc01566e](https://doi.org/10.1039/c4gc01566e).

30 P. Lignier, R. Bellabarba and R. P. Tooze, Scalable Strategies for the Synthesis of Well-Defined Copper Metal and Oxide Nanocrystals, *Chem. Soc. Rev.*, 2012, 41(5), 1708–1720, DOI: [10.1039/c1cs15223h](https://doi.org/10.1039/c1cs15223h).

31 S. Li, Y. Chen, L. Huang and D. Pan, Large-Scale Synthesis of Well-Dispersed Copper Nanowires in an Electric Pressure Cooker and Their Application in Transparent and Conductive Networks, *Inorg. Chem.*, 2014, 53(9), 4440–4444.

32 Y. Shi, H. Li, L. Chen and X. Huang, Obtaining Ultra-Long Copper Nanowires via a Hydrothermal Process, *Sci. Technol. Adv. Mater.*, 2005, 6(7), 761–765, DOI: [10.1016/j.stam.2005.06.008](https://doi.org/10.1016/j.stam.2005.06.008).

33 R. K. Bheema, J. Gopu, A. V. Praveen Kumar and K. C. Etika, BST@Copper Nanowire/Epoxy Composites with Excellent Microwave Absorption in the X-Band, *Chem. Eng. J.*, 2024, 496, 153760, DOI: [10.1016/j.cej.2024.153760](https://doi.org/10.1016/j.cej.2024.153760).

34 Y. Chang, M. L. Lye and H. C. Zeng, Large-Scale Synthesis of High-Quality Ultralong Copper Nanowires, 2005, vol. 20, pp. 3746–3748.

35 T. Zhang, W. Y. Hsieh, F. Daneshvar, C. Liu, S. P. Rwei and H. J. Sue, Copper(i)-Alkylamine Mediated Synthesis of Copper Nanowires, *Nanoscale*, 2020, 12(33), 17437–17449, DOI: [10.1039/d0nr04778c](https://doi.org/10.1039/d0nr04778c).



36 D. V. Ravi Kumar, I. Kim, Z. Zhong, K. Kim, D. Lee and J. Moon, Cu(Ii)-Alkyl Amine Complex Mediated Hydrothermal Synthesis of Cu Nanowires: Exploring the Dual Role of Alkyl Amines, *Phys. Chem. Chem. Phys.*, 2014, **16**(40), 22107–22115, DOI: [10.1039/c4cp03880k](https://doi.org/10.1039/c4cp03880k).

37 Y. Zheng, N. Chen, C. Wang, X. Zhang and Z. Liu, Oleylamine-Mediated Hydrothermal Growth of Millimeter-Long Cu Nanowires and Their Electrocatalytic Activity for Reduction of Nitrate, 2018, *Nanomaterials*, 2018, **8**(4), 192, DOI: [10.3390/nano8040192](https://doi.org/10.3390/nano8040192).

38 H. Ruan, R. Wang, Y. Luo and H. Liu, Study on Synthesis and Growth Mechanism of Copper Nanowires *via* a Facile Oleylamine-Mediated Process, *J. Mater. Sci. Mater. Electron.*, 2016, **27**(9), 9405–9409, DOI: [10.1007/s10854-016-4984-5](https://doi.org/10.1007/s10854-016-4984-5).

39 R. Javed, A. Sajjad, S. Naz, H. Sajjad and Q. Ao, Significance of Capping Agents of Colloidal Nanoparticles from the Perspective of Drug and Gene Delivery, Bioimaging, and Biosensing : An Insight, *Int. J. Mol. Sci.*, 2022, **23**(18), 10521.

40 A. Parkash, Effects of Capping Agents on Shape , Stability , and Oxygen Evolution Reaction Activity of Copper Nanoparticles Effects of Capping Agents on Shape, *Stability, and Oxygen Evolution Reaction Activity of Copper Nanoparticles*, DOI: [10.1149/2754-2734/acb500](https://doi.org/10.1149/2754-2734/acb500).

41 W. Xu, L. Wang, Z. Guo, X. Chen, J. Liu, X. Huang, B. F. Matreials, S. Devices, I. Machines and C. Academy, Copper Nanowires as Nanoscale Interconnects : Their Stability, *Electrical Transport , and Mechanical*, 2015, **1**, pp. 241–250.

42 Y. Zheng, N. Chen, C. Wang, X. Zhang and Z. Liu, Oleylamine-Mediated Hydrothermal Growth of Millimeter-Long Cu Nanowires and Their Electrocatalytic Activity for Reduction of Nitrate, *Nanomaterials*, 2018, **8**(4), 192, DOI: [10.3390/nano8040192](https://doi.org/10.3390/nano8040192).

43 Y. Zhao, Y. Zhang, Y. Li, Z. He and Z. Yan, Rapid and Large-Scale Synthesis of Cu Nanowires *via* a Continuous Flow Solvothermal Process and Its Application in Dye-Sensitized Solar Cells (DSSCs), *RSC Adv.*, 2012, **2**(30), 11544–11551, DOI: [10.1039/c2ra21224b](https://doi.org/10.1039/c2ra21224b).

44 Z. Yin, C. Lee, J. Yoo and Y. Piao, Facile Synthesis of Oxidation-Resistant Copper Nanowires toward Solution-Processable, Flexible Foldable and Free-Standing Electrodes, *Small*, 2014, **10**(24), 5047–5052, DOI: [10.1002/smll.201401276](https://doi.org/10.1002/smll.201401276).

45 N. Shukla, C. Liu, P. M. Jones and D. Weller, FTIR Study of Surfactant Bonding to FePt Nanoparticles, 2003, *J. Magn. Magn. Mater.*, 2003, **266**(1–2), 178–184, DOI: [10.1016/S0304-8853\(03\)00469-4](https://doi.org/10.1016/S0304-8853(03)00469-4).

46 S. Ramya, D. Nataraj, S. Krishnan, S. Premkumar, T. Thrupthika and A. Sangeetha, Aggregation Induced Emission Behavior in Oleylamine Acetone System and Its Application to Get Improved Photocurrent from -, *Sci. Rep.*, 2020, **1**–16, DOI: [10.1038/s41598-020-76703-0](https://doi.org/10.1038/s41598-020-76703-0).

47 F. Lan, J. Bai and H. Wang, The Preparation of Oleylamine Modified Micro-Size Sphere Silver Particles and Its Application in Crystalline Silicon Solar Cells, *RSC Adv.*, 2018, **8**(30), 16866–16872, DOI: [10.1039/c8ra02620c](https://doi.org/10.1039/c8ra02620c).

48 N. Jardón-Maximino, M. Pérez-Alvarez, R. Sierra-Ávila, C. A. Ávila-Orta, E. Jiménez-Regalado, A. M. Bello, P. González-Morones and G. Cadenas-Pliego, Oxidation of Copper Nanoparticles Protected with Different Coatings and Stored under Ambient Conditions, *J. Nanomater.*, 2018, **2018**, 9512768, DOI: [10.1155/2018/9512768](https://doi.org/10.1155/2018/9512768).

49 T. Zhang, M. Zhao, F. Daneshvar, F. Xia and H. J. Sue, Solution-Processable Oxidation-Resistant Copper Nanowires Decorated with Alkyl Ligands, *ACS Appl. Nano Mater.*, 2019, **2**(12), 7775–7784, DOI: [10.1021/acsanm.9b01819](https://doi.org/10.1021/acsanm.9b01819).

50 D. Deng, Y. Jin, Y. Cheng, T. Qi and F. Xiao, Copper Nanoparticles: Aqueous Phase Synthesis and Conductive Films Fabrication at Low Sintering Temperature, *ACS Appl. Mater. Interfaces*, 2013, **5**(9), 3839–3846, DOI: [10.1021/am400480k](https://doi.org/10.1021/am400480k).

51 B. Sirichandana, B. G. M. Patel, N. Chattham and G. Hegde, Properties , Synthesis , and Characterization of Cu - Based Nanomaterials, *Copper-Based Nanomater. Org. Transform. Part 1 – Prop.* 2024, **1**–33, DOI: [10.1021/bk-2024-1466.ch001](https://doi.org/10.1021/bk-2024-1466.ch001).

52 R. Hassanien, M. M. Almaky, A. Houlton and B. R. Horrocks, Preparation and Electrical Properties of a Copper-Conductive Polymer Hybrid Nanostructure, *RSC Adv.*, 2016, **6**(101), 99422–99432, DOI: [10.1039/c6ra20325f](https://doi.org/10.1039/c6ra20325f).

53 J. J. Chen, S. L. Liu, H. B. Wu, E. Sowade, R. R. Baumann, Y. Wang, F. Q. Gu, C. R. L. Liu and Z. S. Feng, Structural Regulation of Silver Nanowires and Their Application in Flexible Electronic Thin Films, *Mater. Des.*, 2018, **154**, 266–274, DOI: [10.1016/j.matdes.2018.05.018](https://doi.org/10.1016/j.matdes.2018.05.018).

54 L. Xu, Y. Yang, Z. W. Hu and S. H. Yu, Comparison Study on the Stability of Copper Nanowires and Their Oxidation Kinetics in Gas and Liquid, *ACS Nano*, 2016, **10**(3), 3823–3834, DOI: [10.1021/acsnano.6b00704](https://doi.org/10.1021/acsnano.6b00704).

